LA-UR -79-3332

TITLE: NEUTRON CROSS SECTION CALCULATIONS FOR
FISSION-PRODUCT NUCLEI

AUTHOR(S): E. D. Arthur and D. G. Foster, Jr.

SUBMITTED TO: NEANDC Specialist Meeting on Neutron
Cross Sections of Fission Product Nuclei
Bologna, Italy
December 12-14, 1979

MASTER
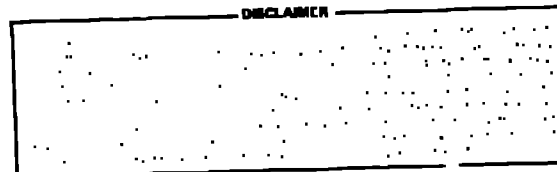
los alamos
scientific laboratory
of the University of California
LOS ALAMOS, NEW MEXICO 87545

An Affirmative Action/Equal Opportunity Employer

NEUTRON CROSS SECTION CALCULATIONS FOR FISSION-PRODUCT NUCLEI

E. D. Arthur and D. G. Foster, Jr.
Los Alamos Scientific Laboratory, University of California
Theoretical Division
Los Alamos, New Mexico 87545

ABSTRACT

To satisfy nuclear data requirements for fission-product nuclei, we performed Hauser-Feshbach statistical calculations with preequilibrium corrections for neutron-induced reactions on isotopes of Se, Kr, Sr, Zr, Mo, Sn, Xe, and Ba between 0.001 and 20 MeV. Spherical neutron optical parameters were determined by simultaneous fits to resonance data and total cross sections. Isospin coefficients appearing in the optical potentials were determined through analysis of the behavior of s- and p-wave strengths as a function of mass for a given Z. Gamma-ray strength functions, determined through fits to stable-isotope capture data, were used in the calculation of capture cross sections and gamma-ray competition to particle emission. The resulting (n,γ), (n,n'), $(n,2n)$, and $(n,3n)$ cross sections, the secondary neutron emission spectra, and angular distributions calculated for 19 fission products will be averaged to provide a resulting ENDF-type fission-product neutronics file.

To provide averaged neutronics information for fission-product nuclei we have performed nuclear-model calculations on a number of nuclei resulting from fast-neutron induced fission of U-235 and Pu-239. To approximate the sum over the constituents of yield curves for fission products, we have chosen a weighted average of the cross sections calculated for a few selected nuclides. These nuclei were chosen from the maximum and half-value points of the yield curves for both low- and high-mass fragments, using distinct sets for U-235 and Pu-239 fission. The resulting 19 nuclides are listed in Table I. We calculated, assuming each of these as a target, cross sections for the (n,γ), (n,n'), $(n,2n)$, and $(n,3n)$ reactions, together with elastic and inelastic angular distributions and neutron emission spectra in the incident neutron energy range beteen 0.001 and 20 MeV.

We relied upon use of the Hauser-Feshbach statistical model/1/ to which we applied preequilibrium corrections necessary at higher energies. This combination of nuclear models has generally worked well in the case of neutron cross-section calculations on stable nuclei, once suitable input parameters have been determined. We did not include direct-reaction effects since these contributions make up a comparatively small part of the total

TABLE I

NUCLIDES USED FOR FISSION PRODUCT CALCULATIONS

	U-235	Pu-239
Lower Peak		
Low	^{87,88}Se	^{92,93}Kr
Center	^{94,95}Sr	^{99,100}Zr
High	^{102,103}Zr	^{107,108}Mo
Higher Peak		
Low	^{131}Sn	^{130}Sn
Center	^{138,139}Xe	^{137,138}Xe
High	^{146}Ba	^{145}Ba

reaction cross section. We sought to improve the reliability of the calcu-
lated results obtained from these models through a careful determination of
input parameters. Generally we fitted various types of stable-isotope experi-
mental data and then tried to determine means by which to extrapolate these
parameter sets for use with unstable target nuclei. We further checked the
applicability of these input parameters through comparison of calculated
cross sections, such as those for (n,2n) reactions, to experimental results.

Special attention was paid to the determination of spherical neu-
tron optical parameters suitable for use over the major portion of the inci-
dent energy range. The use of optical parameters that simultaneously describe
lower and higher energy data is important for the calculation of (n,xn)
reactions where accurate compound-nucleus formation cross sections are needed
at higher energies along with a reasonable description of the emission of
low energy neutrons. We followed the "SPRT"/2/ approach in which total cross-
section data available over a wide energy range were used with low-energy res-
onance data in a simultaneous fit. For extrapolation to neutron-rich nuclei,
we included isospin terms in both the real and imaginary potential. The coef-
ficients V_1, W_1 multiplying the $\eta \equiv \frac{(N-Z)}{A}$ terms were determined through fits to
the behavior of experimental s- and p-wave strength values as a function of η
for a given Z. As an example, Fig. 1 illustrates our fit to xenon total-cross
section data while Fig. 2 compares our calculated s-wave strength-function
values to experimental data for xenon isotopes having differing Z values. The
xenon optical parameters along with those determined for other nuclei involved
in these calculations appear in Table II. The V_1 and W_1 coefficients shown
in Table II are generally larger than those determined from fits to data such
as elastic scattering from separated isotopes in the MeV region./3/ The
cause for this discrepancy is not clear, but such values are in agreement with
results obtained through similar analyses by Newstead and Delaroche./4/

For calculation of capture cross sections as well as to describe
gamma-ray competition to particle emission, we chose to base gamma-ray trans-
mission coefficients on determined values of the gamma-ray strength function
rather than to normalize them to the ratio $\frac{2\pi<\Gamma_\gamma>}{<D>}$, where $<\Gamma_\gamma>$ and $<D>$ are the
average gamma-ray width and spacing for s-wave resonances. For unstable nu-
clei the $<\Gamma_\gamma>$ and $<D>$ values would have to be deduced from their systematic
behavior over the mass region of interest. Use of the gamma-ray strength
function $f(\varepsilon_\gamma)$ defined by

TABLE II

SPHERICAL OPTICAL PARAMETERS[a]

Element	V_0	V_1	α	r_r	a_r	W_0	W_1	β	r_i	a_1	W_0'
Se	54.8	43	−0.35	1.24	0.62	12.5	33	0.36	1.26	0.65	14.5
Kr	52.75	22	−0.34	1.24	0.62	10.1	35	0.5	1.26	0.65	13.5
Sr	49.4	0	−0.15	1.24	0.62	8.5	36	0.5	1.26	0.58	12.9
Zr	48.6	0	−0.33	1.24	0.62	7.9	35	0.3	1.26	0.58	11
Mo	50.8	17	−0.22	1.24	0.62	4.8	7	0.45	1.26	0.58	9.75 (Ref. 5)
Sn	56.3	50	−0.28	1.25	0.57	4.4	15	0.5	1.25	0.56	9.5
Xe	55.4	50	−0.35	1.25	0.65	12.8	50	0.4	1.25	0.56	17.1
Ba	49.0	22	−0.15	1.25	0.74	7.8	32	0.48	1.25	0.58	13

---

[a]Real and imaginary (Saxon derivative) forms used were

$$V = V_0 - V_1 \eta + \alpha E$$

$$W = W_0 - W_1 \eta + \beta E$$

$$W_{max} = W_0' - W_1 \eta, \quad \text{with } V \text{ and } W \text{ in MeV}; r_r, a_r, r_i, \text{ and } a_1 \text{ in fm.}$$

Spin orbit values used were

$$V_{SO} = 6.2 \text{ MeV}, \quad r_{SO} = 1.12 \text{ fm}, \quad a_{SO} = 0.47 \text{ fm for Se, Kr, Sr, Zr, Mo isotopes.}$$

$$V_{SO} = 7.5 \text{ MeV}, \quad r_{SO} = 1.25 \text{ fm}, \quad a_{SO} = 0.65 \text{ fm for Sn, Xe, and Ba, isotopes.}$$
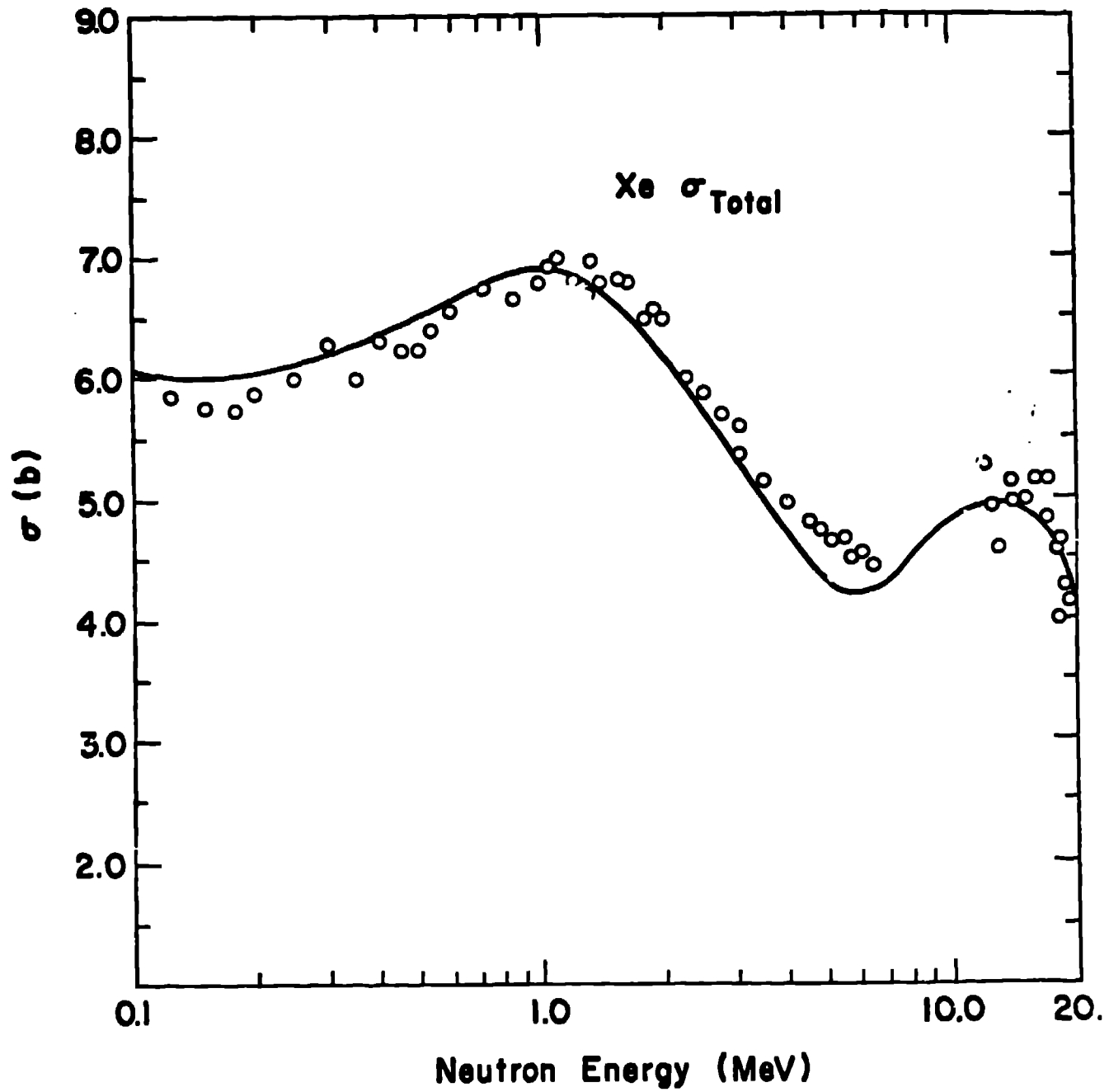
Fig. 1.

Comparison of calculated and experimental values for the
xenon total cross section.
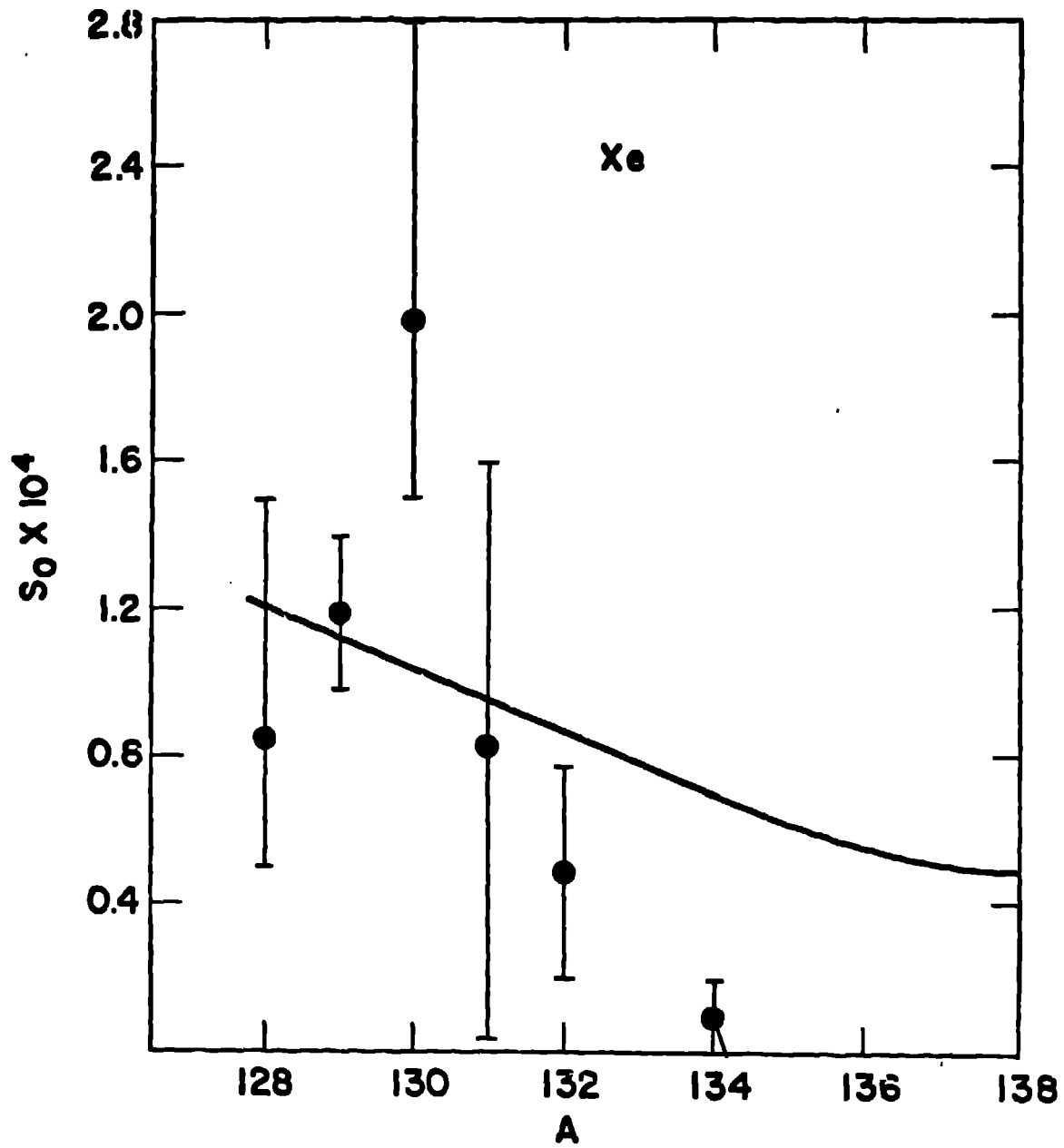
Fig. 2.

Calculated and experimental dependence of the s-wave strength function S_0 for isotopes of xenon.

$$\frac{<\Gamma_\gamma>}{<D>} = \int_0^{S_n} f(\epsilon_\gamma)\, \epsilon_\gamma^3\, \rho(S_n-\epsilon_\gamma)d\epsilon_\gamma \quad , \tag{1}$$

where S_n is the neutron separation energy and   is the compound system level density, eliminates much of this uncertainty. If the strength function is assumed to have a giant dipole resonance form given by

$$f_{E1}(\epsilon_\gamma) = \frac{k\epsilon_\gamma \Gamma_{GDR}}{(\epsilon_\gamma \Gamma_{GDR})^2 + (\epsilon_\gamma^2 - E_{GDR}^2)^2} \quad , \tag{2}$$

then the constant appearing in Eq. (2) can be determined from fits to capture cross sections and spectra available for stable isotopes. This strength function should not vary as rapidly as $\frac{2\pi<\Gamma_\gamma>}{<D>}$; thus one can extrapolate its use to neutron-rich nuclei with greater confidence. As an example, Fig. 3 illustrates calculated gamma-ray strength functions for various Sn compound systems as determined from fits to capture data on Sn-116, Sn-118, Sn-119, and Sn-120. The extracted strength function varies at most by about 50%, a part of which may result from the fact that recent capture measurements in the keV region do not exist for these nuclei. On the other hand, the $\frac{2\pi<\Gamma_\gamma>}{<D>}$ ratios vary by a much larger amount, ranging from values of 0.0003 for n + Sn-120 to 0.013 for n + Sn-119. Figure 3 illustrates the range covered by strength functions determined for representative nuclei in this work.

Additional parameters needed for the present calculations included discrete level data, level-density information, and preequilibrium parameters. Some discrete level information was available from experimental measurements that was augmented in some cases by information based on shell model arguments./6/ To represent the continuum region where no discrete level information existed, we used the Gilbert-Cameron level density expressions/7/ with the Cook parameters/8/ as obtained from a systematic study of resonance spacings near the neutron binding energy. Preequilibrium corrections were applied using the Kalbach master equations model./9/

At low energies we used the COMNUC/10/ Hauser-Feshbach statistical code with the inclusion of width fluctuation corrections. At higher energies the preequilibrium-statistical model code GNASH/11/ was used to calculate cross sections and spectra resulting from multistep reactions. Figure 5 illustrates some of the preliminary calculations we made to further check our input parameter values. Here our calculated values are compared to experimental data for the Zr-90(n,2n) and Sn-112(n,2n) reactions.

Figures 6 and 7 illustrate calculated results for several major neutron reactions on Xe-138 and Xe-139 (solid and dashed curves, respectively). As shown in Table I, we calculated cross sections for both even and odd isotopes of a given element so that the final results, averaged over both cross section sets, would not be biased by such odd-even effects. The capture cross sections calculated in Fig. 6 used the same gamma-ray strength function. The principal reason for the different low-energy cross-section values is the differing neutron separation energies for these two isotopes. The capture cross section for Xe-139 becomes smaller than that for Xe-138 above 0.2 MeV because of competition from inelastic scattering off low-lying states in Xe-139. Most dissimilarities in cross-section shapes shown in Fig. 7 occur because of threshold differences resulting from the odd-even character of these two
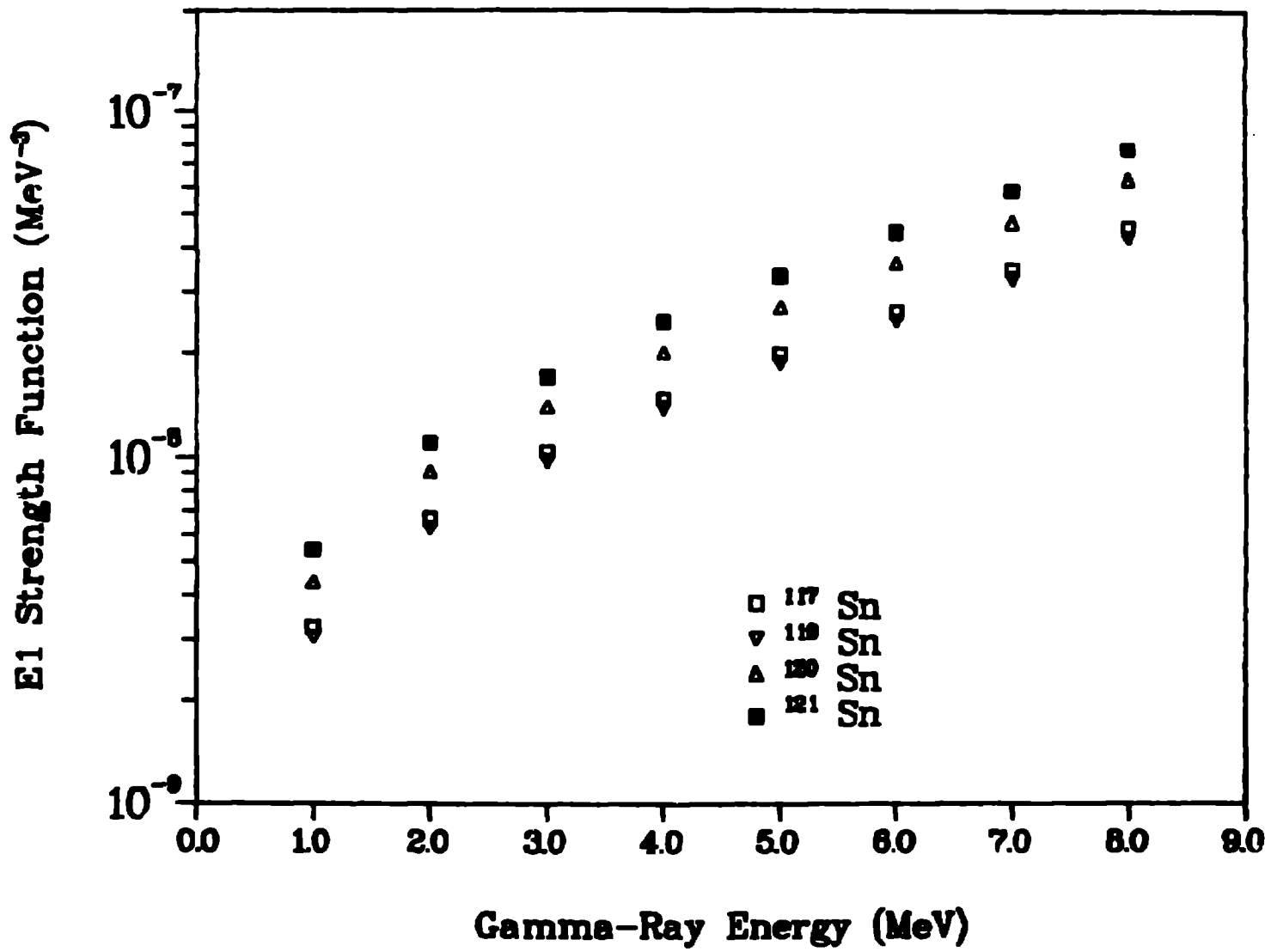
Fig. 3.

Gamma-ray strength functions determined from fits to capture data on tin isotopes.
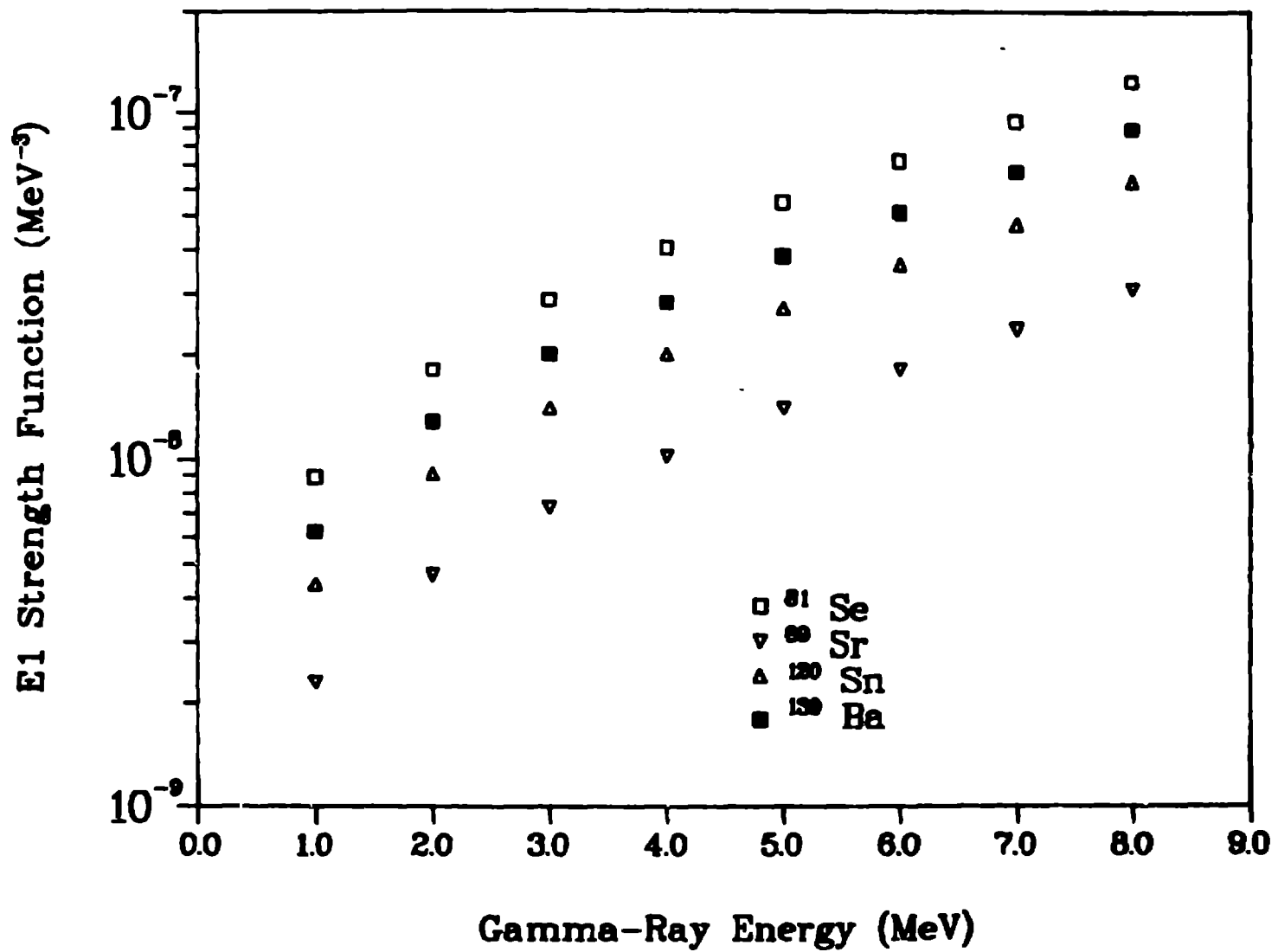
Fig. 4.

Representative gamma-ray strength fui   ons used in this work.
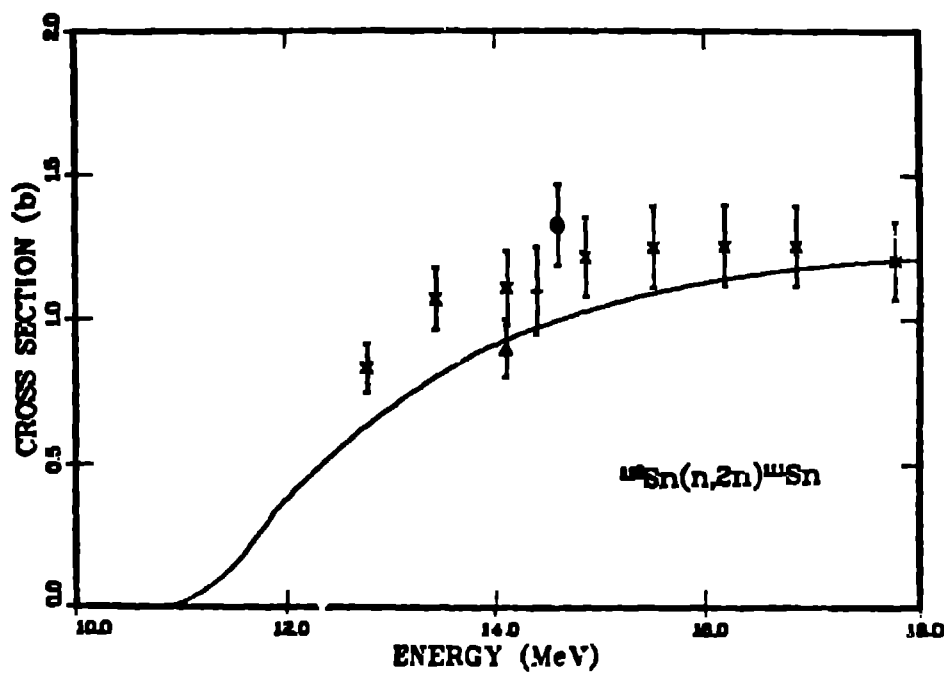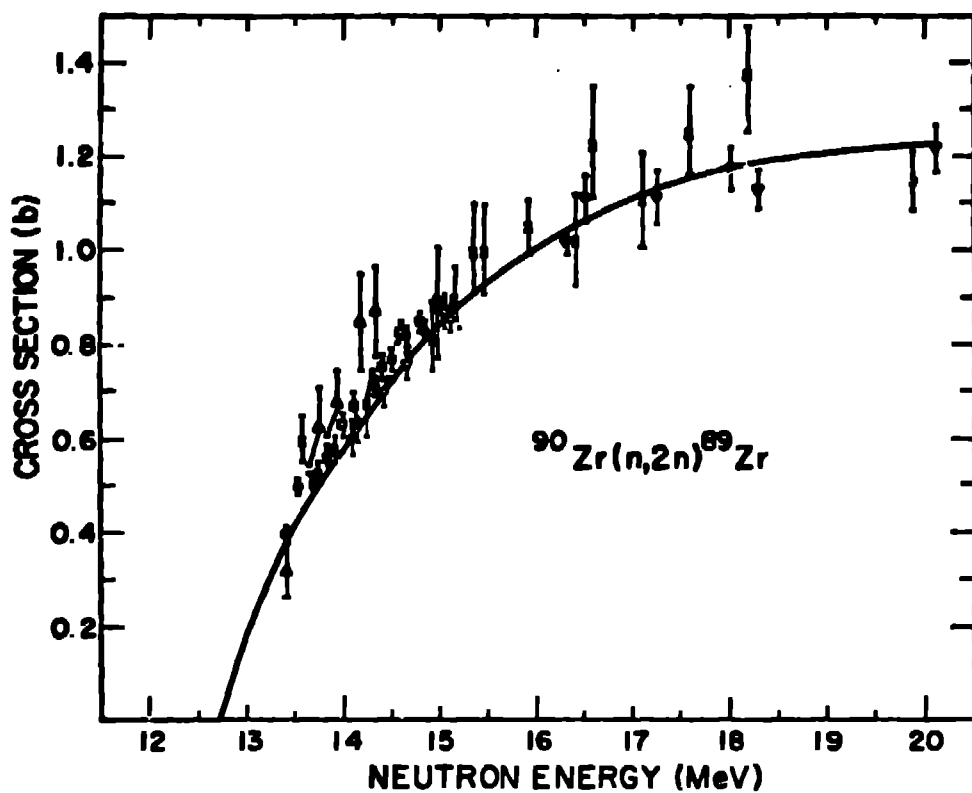
Fig. 5.

Comparison of calculated cross sections to experimental data for the
Zr-90(n,2n) and Sn-112(n,2n) reactions.
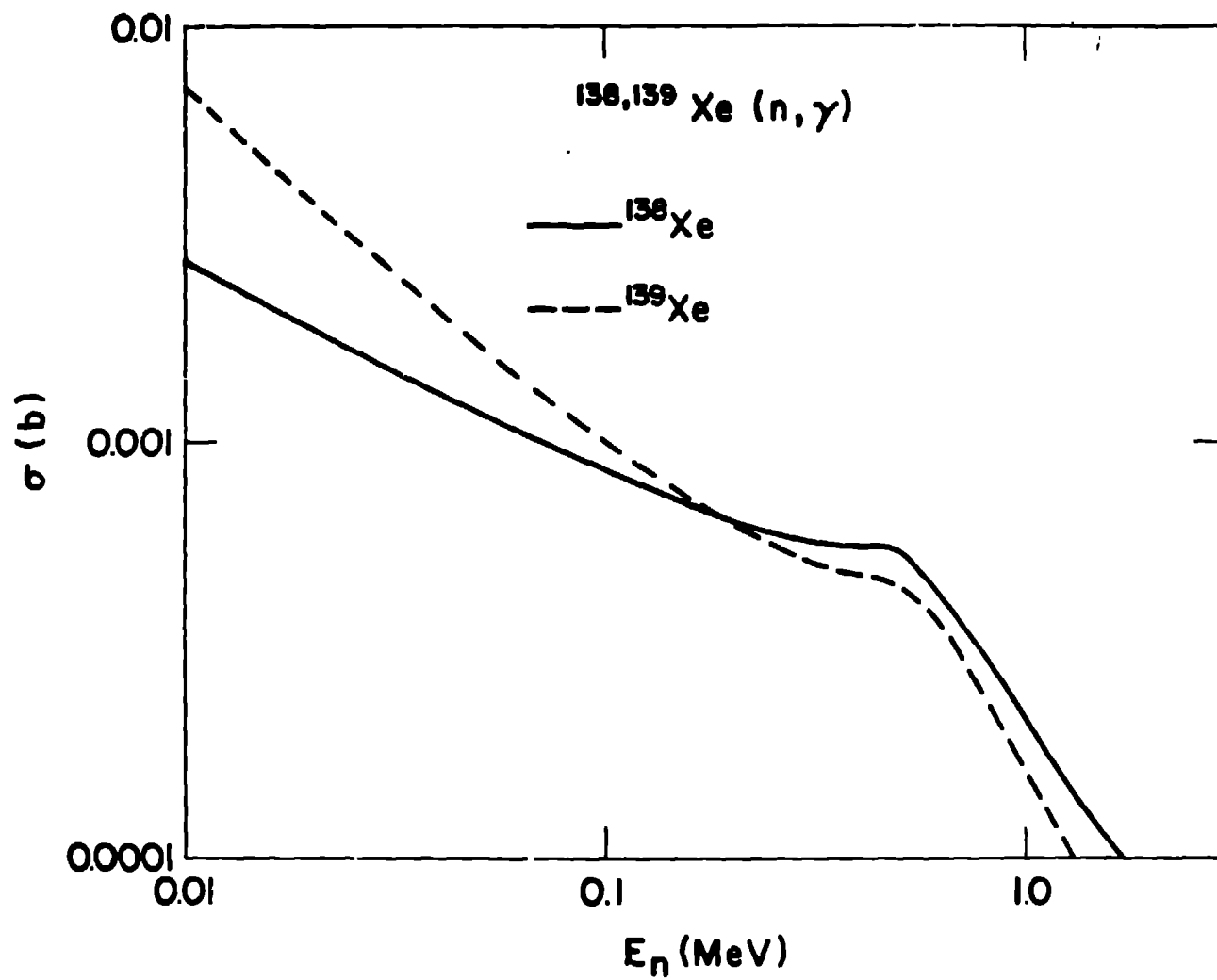
Fig. 6.

Predicted neutron capture cross sections for Xe-138 and Xe-139.
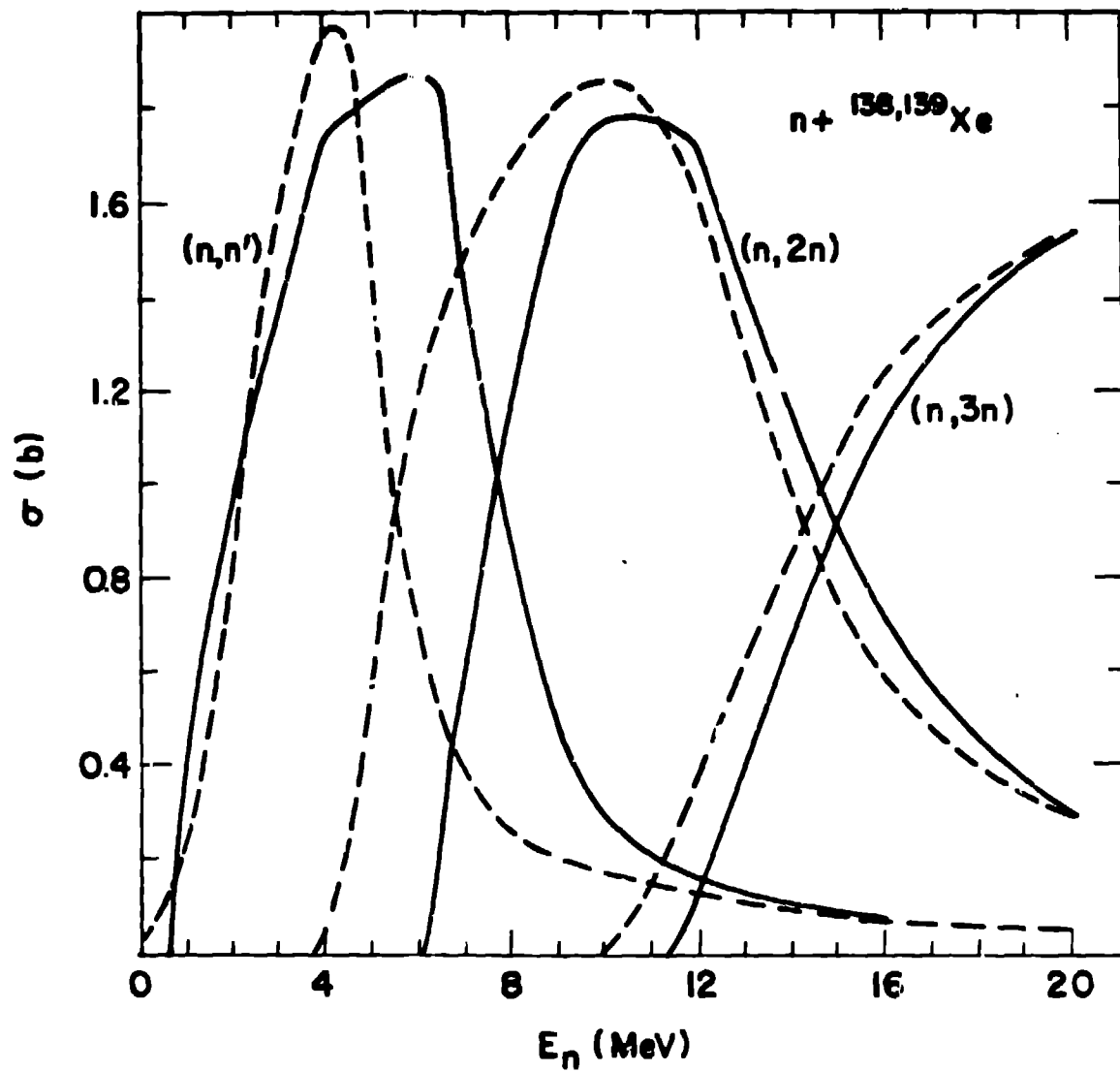
Fig. 7.

A comparison of (n,n'), (n,2n), and (n,3n) cross sections
calculated for Xe-138 and Xe-139 (solid and dashed curves,
respectively).

isotopes. Preequilibrium effects are apparent in that the higher energy portions of the (n,n') and (n,2n) cross sections have higher values than would be obtained from pure Hauser-Feshbach calculations. This in turn decreases the peak values obtained for the calculated (n,2n) and (n,3n) cross sections.

Similar calculations have been completed for all nuclei listed in Table I. Presently we are assembling cross sections, spectra, and angular distributions which will be averaged to produce an ENDF-like file for neutron reaction properties on prompt fission products.

REFERENCES

1. W. Hauser and H. Feshbach, Phys. Rev. 87, 366 (1952).

2. J. P. Delaroche, Ch. Lagrange, and J. Salvy, "Nuclear Theory in Neutron Nuclear Data Evaluation," IAEA-190, 251 (1976).

3. J. D. Ferrer, J. D. Carlson, and J. Rapaport, Nucl. Phys. A275, 325 (1977).

4. C. M. Newstead and J. P. Delaroche, in Nuclear Structure Study with Neutrons, edited by J. Ero and J. Szucs, Budapest (Plenum Press, NY, 1974) p. 142.

5. Ch. Lagrange, Second Advisory Group Meeting on Fission Product Nuclear Data, Petten (Sept. 1977).

6. D. Madland, Los Alamos Scientific Laboratory, personal communication (1979).

7. A. Gilbert and A. G. W. Cameron, Can. J. Phys. 43, 1446 (1965).

8. J. L. Cook, H. Ferguson, and A. R. de L. Musgrove, Aust. J. Phys. 20, 477 (1967).

9. C. Kalbach, Z. Phys. A287, 319 (1978).

10. C. L. Dunford, Atomics International Report AI-AE-12931 (1970).

11. P. G. Young and E. D. Arthur, Los Alamos Scientific Laboratory report LA-6947 (1977).